Title

Alpha Particle Enhanced Blood Brain/Tumor Barrier Permeabilization in Glioblastomas Using Integrin Alpha-v Beta-3–Targeted Liposomes

Journal

Molecular Cancer Therapeutics, 16(10)

ISSN

1535-7163

Authors

Sattiraju, Anirudh
Xiong, Xiaobing
Pandya, Darpan N
et al.

Publication Date

2017-10-01

DOI

10.1158/1535-7163.mct-16-0907

Peer reviewed

HHS Public Access

Author manuscript

Mol Cancer Ther. Author manuscript; available in PMC 2018 October 01.

Published in final edited form as:

Mol Cancer Ther. 2017 October ; 16(10): 2191–2200. doi:10.1158/1535-7163.MCT-16-0907.

Alpha particle enhanced Blood Brain/Tumor Barrier permeabilization in glioblastomas using integrin alpha-v beta-3 targeted liposomes

Anirudh Sattiraju[1], **Xiaobing Xiong**[1], **Darpan N Pandya**[2], **Thaddeus J Wadas**[1,2], **Ang Xuan**[3], **Yao Sun**[1], **Youngkyoo Jung**[1], **Kiran Kumar Solingapuram Sai**[1], **Jay F Dorsey**[4], **King C Li**[1], and **Akiva Mintz**[1,‡]

[1]Department of Radiology, Wake Forest School of Medicine, Winston-Salem, NC 27157, USA

[2]Department of Cancer Biology, Wake Forest School of Medicine, Winston-Salem, NC 27157, USA

[3]Department of Nuclear Medicine and Radiology, the People's Hospital of Zhengzhou University, Zhengzhou, Henan 450003, China

[4]Department of Radiation Oncology, Perelman School of Medicine, University of Pennsylvania, Philadelphia, PA 19104, USA

Abstract

Glioblastoma (GBM) is the most common primary malignant astrocytoma characterized by extensive invasion, angiogenesis, hypoxia and micrometastasis. Despite the relatively leaky nature of GBM blood vessels, effective delivery of anti-tumor therapeutics has been a major challenge due to the complications caused by the blood brain barrier (BBB) and the highly torturous nature of newly formed tumor vasculature (blood tumor barrier-BTB). External beam radiation therapy was previously shown to be an effective means of permeabilizing central nervous system (CNS) barriers. By using targeted short ranged radionuclides, we show for the first time that our targeted actinium-225 labeled $\alpha_v\beta_3$-specific liposomes (^{225}Ac-IA-TLs) caused catastrophic double stranded DNA breaks and significantly enhanced the permeability of BBB and BTB in mice bearing orthotopic GBMs. Histological studies revealed characteristic α-particle induced double strand breaks within tumors but was not significantly present in normal brain regions away from the tumor where BBB permeability was observed. These findings indicate that the enhanced vascular permeability in these distal regions did not result from direct α-particle induced DNA damage. Based on these results, in addition to their direct anti-tumor effects, ^{225}Ac-IA-TLs can potentially be used to enhance the permeability of BBB and BTB for effective delivery of systemically administered anti-tumor therapeutics.

Keywords

Alpha particle radiotherapy; Blood brain-tumor barrier; Glioblastoma; Integrin $\alpha_v\beta_3$; Drug delivery

‡**Address all correspondence to:** Akiva Mintz, MD, PhD, MHA, Wake Forest Baptist Medical Center, 1 Medical Center Blvd, Winston-Salem, NC 27157. amintz@wakehealth.edu.

INTRODUCTION

Glioblastoma (GBM) is the most common and aggressive primary malignant astrocytoma which accounts for nearly 15,000 deaths annually (1). GBMs are characterized by infiltrating margins, angiogenesis and micrometastasis which result in residual disease that persists even after treatment, giving rise to aggressive tumors which are often resistant to standard therapy (2–4). Surgical resection, external beam radiotherapy and conventional chemotherapy only improve patient survival by a few months. Importantly, many chemotherapies and systemically administered anti-GBM therapies which have been shown to be very effective *in vitro* are not effective in the clinic due to their poor and non-uniform distribution within the central nervous system (CNS) (5,6).

The Blood Brain Barrier (BBB) is a protective vascular architecture shown to complicate the effective diffusion of systemically administered therapies into the CNS for treating various neurological disorders (7–13). Therefore, significant efforts are being made to design safe and sophisticated strategies to bypass such barriers for efficient drug delivery (14–17). Multiple recent studies have shown that exposure to external beam radiation enhances BTB permeability in mice bearing orthotopic GBMs (18–22). These studies highlight the effect of ionizing radiation on the permeability of the BTB and the potential of using targeted molecular radiotherapeutics for this purpose with the added benefit of limiting collateral damage to healthy brain tissue. α-particle irradiation is characterized by a short range (50–100μm) and high linear energy transfer (~80keV/μm) which causes irreparable DNA double strand breaks. Actinium (^{225}Ac) is effective for use in such strategies due to its 10 day half-life and the release of four α-particles upon its decay (23). Targeting α-particles towards tumor specific cell surface receptors can spare healthy brain tissue surrounding tumors (24). While we and others have demonstrated the potential of using targeted β-emitting radiotherapy (25), its relatively long range energy and significantly lower killing potential make β-emitting radioisotopes less attractive than α-particle emitters in resistant brain cancers that exist in the immediate vicinity of normal brain.

Tumors are characterized by extensive accumulation of fluid due to leaky blood vessels resulting from disorganized angiogenic endothelial cells and lack effective lymphatic drainage (26). This property of tumors, termed Enhanced Permeability and Retention (EPR), allows nanoparticles to passively accumulate within tumor tissue. By targeting liposomes, we can not only deliver nanoparticles to tumor tissue passively by EPR, but also actively target them to tumor specific cell surface receptors resulting in their retention and internalization (27–29).

The purpose of this work is to demonstrate the effectiveness of ^{225}Ac-labeled targeted liposomes (^{225}Ac-TL) to both enhance the BBB/BTB permeability to systemically delivered agents as well as to elicit characteristic double stranded DNA breaks in tumors. To accomplish these goals, we targeted liposomes to the well characterized integrin alpha-V beta-3 ($\alpha_v\beta_3$), which is not only highly expressed on angiogenic endothelial cells but also on GBM cells at margins of invasion (30,31). We therefore developed a small molecule integrin antagonist (IA) that we previously reported to strongly bind $\alpha_v\beta_3$ integrin and is now in

early stage clinical trials (32–38). We subsequently showed the specificity of our targeted liposomes towards integrin $\alpha_v\beta_3$ using human glioma cell lines and human umbilical cord vascular endothelial cells *in vitro*. This specificity was reinforced by demonstrating binding of IA-TLs to the $\alpha_v\beta_3$ expressing M21 human melanoma cell line but lack of binding to the control matched M21L cell line, which is a stable variant of M21 cell line lacking $\alpha_v\beta_3$ expression (39). Therefore, for this work, we targeted ^{225}Ac-labeled liposomes with IA and examined their effects on enhancing BBB/BTB permeability by evaluating the extravasation of systemically administered albumin binding dye (Evans Blue dye) and MR contrast (Gadopentetic acid) into neural and GBM tissue. Extravasation of Evans Blue dye and gadopentetic acid which have a molecular weight that is similar or higher than that of commonly used chemotherapeutic agents such as temozolomide indicates that our alpha particle based strategy could potentially be used to deliver systemic therapies more effectively to GBMs.

MATERIALS AND METHODS

Animals

Male immunocompetent and athymic nude mice were purchased from Taconic Farms. All colonies were housed in a pathogen-free facility of the Animal Research Program at Wake Forest School of Medicine under a 12:12-h light/dark cycle and fed ad libitum. The institutional IACUC guidelines for the care and use of laboratory animals were followed for all *in vivo* experiments.

Cell culture

U87 MG human GBM cell line was acquired from ATCC in 2008 and cultured in DMEM media (Corning, NY) supplemented with 10% FBS (Invitrogen) and 1% Antibiotic-Antimycotic (Gibco). Early passage cells were cryopreserved in freezing medium containing 5% DMSO (ThemoFisher Scientific). For our experiments, previously cryopreserved early passage U87 MG cells were resuscitated and cultured for 2 weeks before being implanted *in vivo* in athymic nude mice.

Partially polymerized liposomes and Actinium-225

The lipids 1,2-di-(10Z,12Z-tricosadiynoyl)-sn-glycero-3-phosphoethanolamine (DiynePE), 1,2-di-(10Z,12Ztricosadiynoyl)-sn-glycero-3-phosphocholine (DiynePC), and 1,2-dipalmitoyl-sn-glycero-3-phosphocholine (DPPC) were purchased from Avanti Polar Lipids. Inc. (Alabaster, AL) and used without further purification. The radioactive tracer Actinium-225 was obtained from Washington State University at Saint Louis, MO. Functional lipids, 1,2-di-(10Z,12Z-tricosadiynoyl)-sn-glycero-3-phosphoethanolamine with conjugated DOTA (DiynePE-DOTA), 1,2-di-(10Z,12Z-tricosadiynoyl)-sn-glycero-3-phosphoethanolamine-PEG-integrin antagonist (DiynePE-PEG-IA) were synthesized and confirmed by mass spectrometry.

Synthesis of IA- and DOTA-attached polymerizable lipids

To synthesize the monovalent polymerizable IA-lipid, PEG-di(carboxylic acid) linker (HOOC(CH2CH2O)n=2–45COOH) (0.21 mmol) in 15 ml dry dichloromethane was treated

with 1-(3-dimethylaminopropyl)-3-ethylcarbodiimide hydrochloride (EDC) and N-hydroxysuccinimide (NHS) to form NHS ester, which was treated with 1,2-di-(10Z,12Z-tricosadiynoyl)-sn-glycero-3-phosphoethanolamine (DiynePE, 0.1 mmol, Avanti Polar Lipids). The resulted solution was washed with cold brine and purified by a flash chromatography to give pure DiynePE-PEGn-NHS. To the lipid solution of DiynePE-PEGn-NHS (1 mmol) in anhydrous acetonitrile (5 mL), anhydrous dichloromethane (2 mL), and triethylamine (1 mL), IA (1.2 mmol) in DMF was added with continuous stirring in the dark for 24 h. The reaction was complete after stirring at room temperature for 24 hours according to TLC analysis. The reaction solution was evaporated, diluted with water and dialyzed against water using a dialysis bag (cut off size 1000 Da) to give pure DiynePE-PEGn-IA. To synthesize DOTA-attached polymerizable lipid, DiynePE (22.9 μmol) and triethylamine (22.9 μmol) were dissolved in 12 ml of methanol/dichloromethane (10:2, v/v), and S-2-(4-Isothiocyanatobenzyl)-1,4,7,10-tetraazacyclododecane tetraacetic acid (pSCN-Bn-DOTA) (23.0 μmol, Macrocyclics) was added. The reaction mixture was kept under stirring for 24 hours while being protected from light. The reaction solution was washed with brine, dried and precipitate in cold methanol to give pure DiynePE-DOTA.

Radiolabeling of $\alpha_v\beta_3$ targeted IA-TLs with ^{225}Ac

The lipids used in this study include filler lipids (DiynePC and DPPC) and functionalized lipids (DiynePE-DOTA, DiynePE-PEG-IA). TLs were prepared using the same procedure as previously described and the prepared liposomes had a mean diameter of ~ 100 nm. Briefly, lipids were dissolved in 5 ml of chloroform in a 50 ml flask, evaporated under reduced pressure to form thin lipid film. The lipid film was rehydrated to form large vesicles. The lipid solution was then transferred to a 10 ml LIPEX extruder (Northern Lipids Inc., Canada) equipped with two stacked polycarbonate membranes (100 nm pore size) and extruded 10 times at 45°C. The resulting liposomes were then transferred onto a petri dish sitting on ice and irradiated under a 254 nm UV light for an hour to produce liposomes. The liposomes were then filtered using a 220 nm filter followed by purification with Sephadex G50 columns. The nanoparticle size was obtained by dynamic light scattering (DLS) using a Nanosizer (Malvern, UK). For ^{225}Ac labeling, the prepared IA-TL-DOTA was incubated with ^{225}Ac at 70^{o}C for 50 minutes.

Intracranial injection of orthotopic glioblastomas and ^{225}Ac labeled IA-TLs into rodents

Orthotropic GBMs were implanted by stereotactic implantation of 1×10^5 actively growing U87 MG human GBM cells in athymic nude mice. Mice were weighed and anesthetized with a mixture of 114 mg/kg Ketamine and 17 mg/kg xylazine. Mice were then placed in a stereotactic setup and a hole was made 2.0mm lateral and 0.5mm posterior to the bregma in the right cerebral hemisphere through a scalp incision. Stereotactic injection was performed using a Just for Mice stereotaxic apparatus (Harvard Apparatus), with injection of 10-μl syringe (Hamilton) through the hole to a depth of 3.2mm. A Nanomite programmable syringe pump (Harvard Apparatus) delivered constant infusion at a rate of 0.5 μl/min to a total volume of 5 μl.

10 days post tumor implantation, mice received 1μCi of ^{225}Ac-IA-TLs/5μl and 5μg of unlabeled IA-TLs/5μl intracranially using the same procedures that are mentioned above. All

mice received an analgesic (Ketaprofen) and were monitored for body weight, ambulatory, feeding and grooming activities.

Small animal MR imaging

Mice were transported to the Wake Forest small animal imaging facility from the Wake Forest animal housing facility following IACUC approved protocols and anesthetized using a mixture of 114 mg/kg Ketamine and 17 mg/kg xylazine. Mice were then placed on a heating pad and injected with gadopentetic acid intravenously. The mice were then placed on a bed and scanned using a 7 Tesla (7T) MRI scanner. Respiratory rate and temperature of all animals was constantly monitored during the procedure.

Intravenous injection of Evans blue dye and PGLA nanoparticles

Athymic nude rats and mice were anesthetized using isoflurane and placed on a heating pad. The rodent tails were warmed for a few minutes under a heat lamp and Evans Blue dye (2%) diluted in 1X PBS was injected intravenously along with (1μg/μl) of green fluorescing PGLA nanoparticles. The animals were then allowed to recuperate under the heat lamp for a few minutes. After a period of 6 hours, the rodents were anesthetized with a mixture of 114 mg/kg Ketamine and 17 mg/kg xylazine and perfused using IACUC approved protocol.

Extraction and cryopreservation of rodent brains

Anesthetized mice were transcardially perfused with PBS followed by 4% paraformaldehyde (PFA). Extracted brains were postfixed in 4% PFA, cryoprotected in gradients of sucrose, covered with tissue embedding medium, snap frozen in liquid nitrogen and stored at −80 °C.

Tissue Sectioning

Serial, 20 μm thick, transverse sections of the frozen tissues were obtained using a cryostat (Microm HM 500, Zeiss, Germany) at −20°C and were mounted on Super Frost Plus microscope slides (Thermo Scientific) in series of three and were stored at −20 °C.

Immunohistochemistry

Sections were dried at room temperature for an hour, rehydrated in PBS, permeabilized with 0.5 % Triton X-100 (Sigma) in PBS solution and blocked to saturate non-specific antigen sites using 5% (vol/vol) goat serum-PBS (Jackson Immunoresearch Labs) overnight at 4°C. On the next day, the sections were incubated with 0.05% Tween 20 and incubated in anti-γH2A.X antibody (abcam) for 4 hours. Later, the sections were washed using PBS-T and incubated with anti-rabbit Alexa flour 647 for 2 hours in the dark. Later, the sections were imaged on incubated with Hoechst 33342 (nuclear marker). The sections were then mounted using mounting medium and observed under an inverted fluorescence microscope.

Microscopy

An inverted motorized fluorescent microscope (Olympus IX81) with an Orca-R2 Hamamatsu CCD camera (Hamamatsu) and a laser scanning confocal microscope (Olympus FluoView1200) were used for image acquisition. Camera drive and acquisition were

performed using a MetaMorph Imaging System (Olympus, Japan) and Fluo View Viewer 4.2 software (Olympus, Japan) were used for image acquisition.

Image analysis

Images of PLGA fluorescence indicating the permeabilization of the BTB were analyzed using Image J software. ROIs for measuring the area and intensity of extravasated Evans blue dye, PLGA nanoparticles and γH2A.X fluorochrome signal were drawn using Image J software. Olympus Fluo View Viewer 4.2 imaging software was used to analyze fluorescence images.

Statistical analysis

Data are represented as means +/−standard error of mean (SEM). One-way ANOVA (for three or more experimental groups) and Student's t-test were performed to assess if experimental groups were significantly different from each other. All statistical analyses and graphs were generated using GraphPad Prism software. $p<0.05$ was considered to be statistically significant (*).

RESULTS

Development and radiolabeling of IA targeted Liposomes (IA-TLs)

We utilized the liposome formulation previously developed by our group (39). To target our liposomes to GBM and associated vasculature, we conjugated a novel small molecule integrin antagonist (IA) that has been shown to target $\alpha_v\beta_3$ with a high affinity and a more optimal biodistribution compared to peptides (Figure 1A). We used standard DOTA chelation methods to radiolabel our targeted liposome with ^{225}Ac, as we previously reported (Figure 1B) (23,24). Our radiolabeled ^{225}Ac-IA-TL demonstrated uniform size and radiochemical purity (RCP) of 99.6% (Figure 1C).

Cy5.5 labeled IA-TLs show tumor specificity *in vivo*

To demonstrate GBM-specific targeting of our ^{225}Ac-IA-TLs, groups of mice (n=3) bearing $\alpha_v\beta_3$-expressing orthotopic GBMs were intracranially infused with cy5.5 labeled targeted and untargeted liposomes. *In vivo* binding was measured using fluorescence imaging performed 2 days (Figure 2A) and 5 days (Figure 2B) post liposome infusion. Intracranially infused Cy5.5 labeled $\alpha_v\beta_3$ targeted IA-TL accumulated significantly greater within tumor tissue in mice bearing orthotopic GBMs when compared to cy5.5 labeled untargeted liposomes ($p< 0.05$) (Figure 2C). Importantly, Cy5.5-IA-TLs were found to be abundant only within GBM tissue but not in the surrounding normal brain (Figure 2D). This result demonstrated the specificity of targeted IA-TLs towards integrin $\alpha_v\beta_3$ expressing orthotopic tumors and their suitability to test the effects of targeted α-particle radiation on the BBB/BTB permeability.

^{225}Ac-IA-TLs mediates BBB permeability

To examine the targeted α-particle mediated BBB permeability over a period of days, groups of mice (n=3) intracranially infused with ^{225}Ac-IA-TLs were sacrificed 2 days, 5 days and

10 days post-infusion after they were intravenously injected with Evans blue dye. Systemically injected Evans Blue dye does not normally penetrate the BBB and is therefore used to measure permeability of systemically injected agents. We observed modest BBB permeabilization after 2 days and more extensive Evans blue dye extravasation after 5 days, which steadily increased until 10 days post-surgery (Figure 3A). The area of distribution and intensity of Evans blue dye were significantly higher in mice intracranially infused with ^{225}Ac-IA-TLs when compared to control mice (Figure 3B and 3C). Control mice intracranially infused with saline (n=3) only showed minimal Evans Blue dye extravasation after 2 days, likely due to surgical disruption, which completely disappeared at 10 days (Figure 3). These results indicate that ^{225}Ac-IA-TLs cause BBB opening when intracranially infused *in vivo.*

To examine if there was a dose dependent permeability response, we intracranially infused groups of mice (n=5/dose) with 0.05μCi, 0.1μCi or 0.5μCi of ^{225}Ac-IA-TLs. We observed a dose dependent increase in the extravasation of intravenously injected gadopentetic acid (Figure 4A) and Evans Blue dye (Figure 4B). This confirms the potential of using α-particle mediated BBB permeability to deliver systemically administered agents through the BBB.

^{225}Ac labeled IA-TLs enhance BTB permeability in mice bearing orthotopic GBMs

To examine whether α-particle mediated BBB permeability extends to the BTB, we intracranially infused ^{225}Ac-IA-TLs, unlabeled IA-TLs and saline into tumor tissue of mice bearing orthotopic GBMs. Groups of mice (n=3) were sacrificed 2 days and 5 days post ^{225}Ac-IA-TLs infusion, after intravenous injection of Evans Blue dye. We observed increased BTB permeability in mice infused with ^{225}Ac-IA-TLs when compared to mice infused with unlabeled IA-TLs (n=3) (Figure 5A). Upon sectioning the brains, we confirmed the greater area of extravasation of Evans Blue dye in mice intracranially infused with targeted α-particle therapy compared to mice intracranially infused with either unlabeled IA-TLs or saline (Figure 5B and 5C).

Systemic delivery of fluorescent PLGA nanoparticles (300nm) to exploit α-particle enhanced BTB permeabilization

To examine if the α-particle enhanced BTB permeability could be exploited to systemically deliver larger sized agents, we injected fluorescent PLGA nanoparticles (300nm in diameter) into orthotopic GBM-bearing mice treated intratumorally with ^{225}Ac-IA-TLs. Fluorescent PLGA nanoparticles were intravenously injected prior to sacrifice to quantify the accumulation of PLGA nanoparticles within GBMs upon BTB permeabilization. We observed significantly higher accumulation of PLGA nanoparticles within GBM tissue in mice infused with ^{225}Ac-IA-TLs when compared to mice infused with unlabeled IA-TLs (n=3/time point) ($p < 0.05$) (Figure 5D). PLGA fluorescence in and around GBM tissue was normalized to fluorescence signal from contralateral brain regions before analysis. These results demonstrate that ^{225}Ac-IA-TLs also significantly enhance BTB permeability to larger systemically injected agents.

Alpha particle-induced double-stranded DNA breaks observed at infusion site but not in regions further away

To examine the biological effect of targeted α-particle therapy on GBMs at the site of injection and in the surrounding normal brain where we observed enhanced BBB permeability, we infused mice with ^{225}Ac-IA-TLs and stained for double stranded DNA breaks, a hallmark of α-particle therapy. We observed an abundance of double stranded DNA breaks (manifested by γ H2A.X staining) at the site of infusion in all mice intracranially infused with ^{225}Ac-IA-TLs (n=3/time point) but did *not* observe significant double-stranded DNA breaks in the surrounding regions of normal brain (0.5mm from GBM border) that demonstrated increased BBB/BTB permeability away from infusion site (Figure 6A and 6B). γ H2A.X nuclear signal was found to be significantly higher around infusion sites when compared to regions further away (0.5mm from GBM border) at 2 day and 5 day time points ($p < 0.05$) (Figure 6C). In contrast, we observed negligible presence of γ H2A.X nuclear signal within untreated orthotopic GBMs in mice (Figure 6C). These results indicate that the catastrophic double stranded DNA damage only occurred at the site of infusion (within tumors) but not in the surrounding normal brain where we observed enhanced BBB permeability, demonstrating the potential of safely exploiting this property for systemically administered therapies to target the areas of brain surrounding GBMs that contain infiltrating cells responsible for inevitable recurrences.

DISCUSSION

Effective delivery of systemically administered therapeutics to GBMs is a formidable challenge due to the blood-brain/tumor barrier, with most small molecules unable to cross CNS barriers (40–42). Recurrent disease due to micrometastases that escape exposure to therapeutics is a major driver of patient mortality. Designing strategies that allow drugs to reach micrometastatic sites and the tumor microenvironment is therefore imperative (43,44). In this work, we developed a targeted α-particle platform that we demonstrated can target GBM with lethal α-particles and simultaneously enhance BBB and BTB permeability towards systemically administered agents.

In this study, we showed the *in vivo* specificity of our intracranially infused nanoparticles towards integrin $\alpha_v\beta_3$ expressing orthotopic GBMs. Furthermore, we successfully labeled our nanoparticles with actinium-225, a potent α-particle emitter. After intracranially infusing our ^{225}Ac labeled $\alpha_v\beta_3$ targeting nanoparticles (^{225}Ac-IA-TL) using convection enhanced delivery (CED), we observed enhanced BBB/BTB permeability to systemically administered small molecules to larger nanoparticles. CED is a delivery technique that increases the effective penetration of drugs into GBM by forcing fluid into the parenchyma and does not rely on the limited diffusion of drug after bolus injection. This technique has greatly improved over the past few years as novel catheters have been manufactured that overcome the shortcomings of early CED clinical trials (45). In addition to the added permeability to the BTB after delivering ^{225}Ac-IA-TL via CED, we also observed permeability within surrounding normal brain where the micrometastatic invasive disease often remains and causes recurrence. Importantly, these areas of normal brain showing added permeability did *not* demonstrate widespread DNA damage caused by targeted α-

particles, indicating translational relevance. Although tumors are characterized by disorganized and leaky vasculature, the highly torturous nature of the tumor vessels and rigidity of tumor associated stroma make it difficult for drugs to extravasate and diffuse into tumor tissue (46). Our results increase our knowledge of the effects of molecular targeted radiation on BBB/BTB permeability. Furthermore, we are currently studying the translational potential of using targeted α-particles to enhance the delivery of systemically administered drugs which do not cross the BBB, that are currently being used in clinic for other malignancies.

When we examined for the presence of double strand DNA breaks, we observed greater sub-nuclear γ H2A.X accumulation in GBM cells around the infusion site and an absence of γ H2A.X in distal regions of normal brain (0.5mm from GBM border) where enhanced vascular permeability was observed. This demonstrates that even though the presence of double strand DNA breaks are limited to GBM tissue, its effect on BTB/BBB permeability is extended even to areas further away within the normal brain. While not the focus of this work, this demonstrates the potential therapeutic effect of our strategy of using ^{225}Ac-IA-TLs to elicit double strand DNA breaks in GBM tissue but not within normal brain. Further studies are now underway to evaluate the direct therapeutic effect of ^{225}Ac-IA-TLs alone and in combination with systemically administered therapies.

CONCLUSIONS

^{225}Ac-IA-TLs enhanced the permeability of BBB and BTB *in vivo* and elicited double strand DNA breaks within GBMs. These characteristics justify further ongoing studies to validate ^{225}Ac-IA-TLs as a candidate therapeutic that can potentially be exploited to effectively deliver other systemic therapeutics across the BBB and BTB to GBM.

Acknowledgments

We would like to thank Ms. Thuy Smith and Ms. Stephanie Rideout Danner for their help with animal studies and their expertise with tissue extraction and processing. We would also like to thank Ken Grant (Wake Forest cellular imaging shared resource) for his help and expertise.

Financial support for the work: This work was supported by the American Cancer Society mentored research scholar grant 124443-MRSG-13-121-01-CDD (Mintz), the National Institutes of Health grants 1R01CA179072-01A1 (Mintz), R01 CA184091-01 (Li) and P30 CA012197 (Pasche, Comprehensive Cancer Center of Wake Forest University (CCCWFU).

References

1. Reardon DA, Wen PY. Therapeutic advances in the treatment of glioblastoma: rationale and potential role of targeted agents. The oncologist. 2006; 11(2):152–164. [PubMed: 16476836]
2. Bissell MJ, Radisky D. Putting tumours in context. Nature reviews Cancer. 2001; 1(1):46–54. [PubMed: 11900251]
3. Jain RK, di Tomaso E, Duda DG, Loeffler JS, Sorensen AG, Batchelor TT. Angiogenesis in brain tumours. Nat Rev Neurosci. 2007; 8(8):610–622. [PubMed: 17643088]
4. Price SJ, Jena R, Burnet NG, et al. Improved delineation of glioma margins and regions of infiltration with the use of diffusion tensor imaging: an image-guided biopsy study. AJNR American journal of neuroradiology. 2006; 27(9):1969–1974. [PubMed: 17032877]
5. Frosina G. DNA repair and resistance of gliomas to chemotherapy and radiotherapy. Molecular cancer research : MCR. 2009; 7(7):989–999. [PubMed: 19609002]

6. Ramirez YP, Weatherbee JL, Wheelhouse RT, Ross AH. Glioblastoma multiforme therapy and mechanisms of resistance. Pharmaceuticals (Basel, Switzerland). 2013; 6(12):1475–1506.
7. Abbott NJ. Astrocyte-endothelial interactions and blood-brain barrier permeability. Journal of anatomy. 2002; 200(6):629–638. [PubMed: 12162730]
8. Abbott NJ, Patabendige AAK, Dolman DEM, Yusof SR, Begley DJ. Structure and function of the blood–brain barrier. Neurobiology of Disease. 2010; 37(1):13–25. [PubMed: 19664713]
9. Agarwal S, Manchanda P, Vogelbaum MA, Ohlfest JR, Elmquist WF. Function of the Blood-Brain Barrier and Restriction of Drug Delivery to Invasive Glioma Cells: Findings in an Orthotopic Rat Xenograft Model of Glioma. Drug Metabolism and Disposition. 2013; 41(1):33–39. [PubMed: 23014761]
10. Hawkins BT, Davis TP. The Blood-Brain Barrier/Neurovascular Unit in Health and Disease. Pharmacological Reviews. 2005; 57(2):173–185. [PubMed: 15914466]
11. Pardridge WM. The blood-brain barrier: bottleneck in brain drug development. NeuroRx : the journal of the American Society for Experimental NeuroTherapeutics. 2005; 2(1):3–14. [PubMed: 15717053]
12. Persidsky Y, Ramirez SH, Haorah J, Kanmogne GD. Blood–brain Barrier: Structural Components and Function Under Physiologic and Pathologic Conditions. Journal of Neuroimmune Pharmacology. 2006; 1(3):223–236. [PubMed: 18040800]
13. Wolburg H, Lippoldt A. Tight junctions of the blood–brain barrier: development, composition and regulation. Vascular Pharmacology. 2002; 38(6):323–337. [PubMed: 12529927]
14. Etame AB, Diaz RJ, Smith CA, Mainprize TG, Kullervo HH, Rutka JT. Focused ultrasound disruption of the blood brain barrier: a new frontier for therapeutic delivery in molecular neuro-oncology. Neurosurgical focus. 2012; 32(1):E3–E3.
15. Leinenga G, Gotz J. Scanning ultrasound removes amyloid-beta and restores memory in an Alzheimer's disease mouse model. Science translational medicine. 2015; 7(278):278ra233.
16. Liu H-L, Hua M-Y, Chen P-Y, et al. Blood-Brain Barrier Disruption with Focused Ultrasound Enhances Delivery of Chemotherapeutic Drugs for Glioblastoma Treatment. Radiology. 2010; 255(2):415–425. [PubMed: 20413754]
17. Xiong X, Sun Y, Sattiraju A, et al. Remote Spatiotemporally Controlled and Biologically Selective Permeabilization of Blood-Brain Barrier. Journal of controlled release: official journal of the Controlled Release Society. 2015; 217:113–120. [PubMed: 26334482]
18. Baumann BC, Kao GD, Mahmud A, et al. Enhancing the Efficacy of Drug-loaded Nanocarriers against Brain Tumors by Targeted Radiation Therapy. Oncotarget. 2013; 4(1):64–79. [PubMed: 23296073]
19. d'Avella D, Cicciarello R, Angileri FF, Lucerna S, La Torre D, Tomasello F. Radiation-induced blood-brain barrier changes: pathophysiological mechanisms and clinical implications. Acta neurochirurgica Supplement. 1998; 71:282–284. [PubMed: 9779208]
20. Gaber MW, Sabek OM, Fukatsu K, Wilcox HG, Kiani MF, Merchant TE. Differences in ICAM-1 and TNF-alpha expression between large single fraction and fractionated irradiation in mouse brain. International journal of radiation biology. 2003; 79(5):359–366. [PubMed: 12943244]
21. Greene-Schloesser D, Robbins ME, Peiffer AM, Shaw EG, Wheeler KT, Chan MD. Radiation-induced brain injury: A review. Frontiers in oncology. 2012; 2:73. [PubMed: 22833841]
22. Hong JH, Chiang CS, Campbell IL, Sun JR, Withers HR, McBride WH. Induction of acute phase gene expression by brain irradiation. International journal of radiation oncology, biology, physics. 1995; 33(3):619–626.
23. Pandya DN, Hantgan R, Budzevich MM, et al. Preliminary Therapy Evaluation of (225)Ac-DOTA-c(RGDyK) Demonstrates that Cerenkov Radiation Derived from (225)Ac Daughter Decay Can Be Detected by Optical Imaging for In Vivo Tumor Visualization. Theranostics. 2016; 6(5):698–709. [PubMed: 27022417]
24. Wadas TJ, Pandya DN, Solingapuram Sai KK, Mintz A. Molecular Targeted α-Particle Therapy for Oncologic Applications. American Journal of Roentgenology. 2014; 203(2):253–260. [PubMed: 25055256]

25. Nguyen V, Conyers JM, Zhu D, et al. A novel ligand delivery system to non-invasively visualize and therapeutically exploit the IL13Ralpha2 tumor-restricted biomarker. Neuro-oncology. 2012; 14(10):1239–1253. [PubMed: 22952195]
26. Maeda H, Nakamura H, Fang J. The EPR effect for macromolecular drug delivery to solid tumors: Improvement of tumor uptake, lowering of systemic toxicity, and distinct tumor imaging in vivo. Adv Drug Deliv Rev. 2013; 65(1):71–79. [PubMed: 23088862]
27. Acharya S, Sahoo SK. PLGA nanoparticles containing various anticancer agents and tumour delivery by EPR effect. Advanced Drug Delivery Reviews. 2011; 63(3):170–183. [PubMed: 20965219]
28. Blanco E, Shen H, Ferrari M. Principles of nanoparticle design for overcoming biological barriers to drug delivery. Nat Biotech. 2015; 33(9):941–951.
29. Kobayashi H, Watanabe R, Choyke PL. Improving Conventional Enhanced Permeability and Retention (EPR) Effects; What Is the Appropriate Target? Theranostics. 2014; 4(1):81–89.
30. Huang R, Harmsen S, Samii JM, et al. High Precision Imaging of Microscopic Spread of Glioblastoma with a Targeted Ultrasensitive SERRS Molecular Imaging Probe. Theranostics. 2016; 6(8):1075–1084. [PubMed: 27279902]
31. Schnell O, Krebs B, Wagner E, et al. Expression of Integrin α(v)β(3) in Gliomas Correlates with Tumor Grade and Is not Restricted to Tumor Vasculature. Brain Pathology (Zurich, Switzerland). 2008; 18(3):378–386.
32. Burnett CA, Xie J, Quijano J, et al. Synthesis, in vitro, and in vivo characterization of an integrin αvβ3-targeted molecular probe for optical imaging of tumor. Bioorganic & Medicinal Chemistry. 2005; 13(11):3763–3771. [PubMed: 15863003]
33. Chen K, Chen X. Integrin Targeted Delivery of Chemotherapeutics. Theranostics. 2011; 1:189–200. [PubMed: 21547159]
34. Hsu AR, Veeravagu A, Cai W, Hou LC, Tse V, Chen X. Integrin alpha v beta 3 antagonists for anti-angiogenic cancer treatment. Recent patents on anti-cancer drug discovery. 2007; 2(2):143–158. [PubMed: 18221059]
35. Kim YS, Li F, Kong R, et al. Multivalency of non-peptide integrin alphaVbeta3 antagonist slows tumor growth. Molecular pharmaceutics. 2013; 10(10):3603–3611. [PubMed: 23961901]
36. Lim EH, Danthi N, Bednarski M, Li KC. A review: Integrin alphavbeta3-targeted molecular imaging and therapy in angiogenesis. Nanomedicine : nanotechnology, biology, and medicine. 2005; 1(2):110–114.
37. Liu Z, Wang F, Chen X. Integrin α(v)β(3)-Targeted Cancer Therapy. Drug development research. 2008; 69(6):329–339. [PubMed: 20628538]
38. Qin G, Li Z, Xia R, et al. Partially polymerized liposomes: stable against leakage yet capable of instantaneous release for remote controlled drug delivery. Nanotechnology. 2011; 22(15):155605. [PubMed: 21389566]
39. Xiong X, Fung S, Tung C-H, Li KC. Partially Polymerized Liposomes for Targeted Drug Delivery, Controlled Drug Release and Molecular Imaging. WMIS annual meeting. 2013
40. Dubois LG, Campanati L, Righy C, et al. Gliomas and the vascular fragility of the blood brain barrier. Frontiers in Cellular Neuroscience. 2014; 8(418)
41. van Tellingen O, Yetkin-Arik B, de Gooijer MC, Wesseling P, Wurdinger T, de Vries HE. Overcoming the blood-brain tumor barrier for effective glioblastoma treatment. Drug resistance updates : reviews and commentaries in antimicrobial and anticancer chemotherapy. 2015; 19:1–12. [PubMed: 25791797]
42. Wolburg H, Noell S, Fallier-Becker P, Mack AF, Wolburg-Buchholz K. The disturbed blood-brain barrier in human glioblastoma. Molecular aspects of medicine. 2012; 33(5–6):579–589. [PubMed: 22387049]
43. Hurst RE, Bastian A, Bailey-Downs L, Ihnat MA. Targeting dormant micrometastases: rationale, evidence to date and clinical implications. Therapeutic Advances in Medical Oncology. 2016; 8(2): 126–137. [PubMed: 26929788]
44. Rulseh AM, Keller J, Klener J, et al. Long-term survival of patients suffering from glioblastoma multiforme treated with tumor-treating fields. World Journal of Surgical Oncology. 2012; 10(1):1–6. [PubMed: 22214417]

45. Debinski W, Tatter SB. Convection-enhanced delivery for the treatment of brain tumors. Expert review of neurotherapeutics. 2009; 9(10):1519–1527. [PubMed: 19831841]

46. Anderson JC, McFarland BC, Gladson CL. New molecular targets in angiogenic vessels of glioblastoma tumours. Expert reviews in molecular medicine. 2008; 10:e23. [PubMed: 18684337]

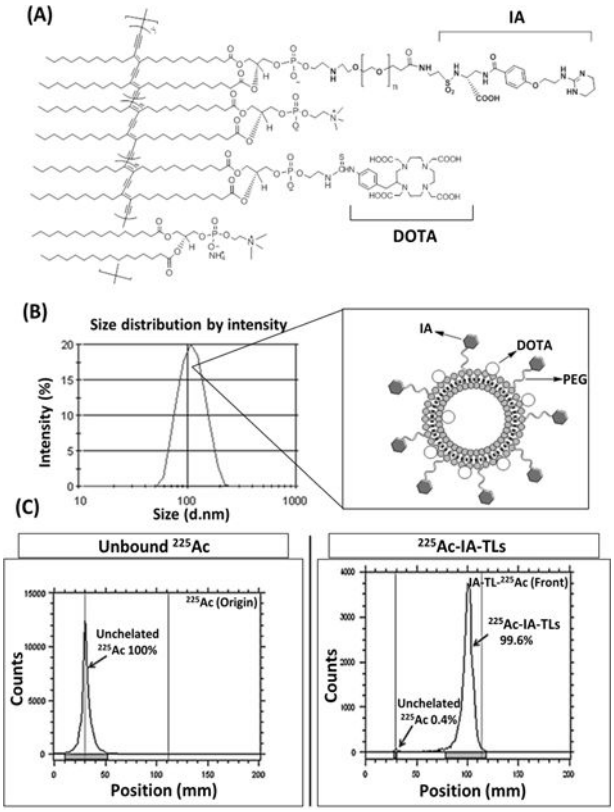

Figure 1. Development of ^{225}Ac labeled $\alpha_v\beta_3$ targeted liposomes (^{225}Ac-IA-TLs)

(A) PEG-di (carboxylic acid) linker (HOOC(CH2CH2O)n=2-45COOH) was conjugated to 1-(3-dimethylaminopropyl)-3-ethylcarbodiimide hydrochloride (EDC) and N-hydroxysuccinimide (NHS) to yield pure DiynePE-PEGn-NHS. Monovalent polymerizable IA-lipid was produced by conjugating IA with lipid solution of DiynePE-PEGn-NHS. (B) TLC analysis showing production of pure DiynePE-PEGn-IA along with diagrammatic representation of IA-TLs; prepared liposomes had a mean diameter of ~100 nm. (C) DiynePE was mixed with S-2-(4-Isothiocyanatobenzyl)-1,4,7,10-tetraazacyclododecane tetraacetic acid (pSCN-Bn-DOTA) to produce pure DiynePE-DOTA. For ^{225}Ac labeling, prepared IA-DOTA-TLs were incubated with ^{225}Ac at 70^{o}C for 50 minutes. Radio-TLC analysis showed effective radiolabeling of targeted liposomes with a radiochemical purity of 99.6%.

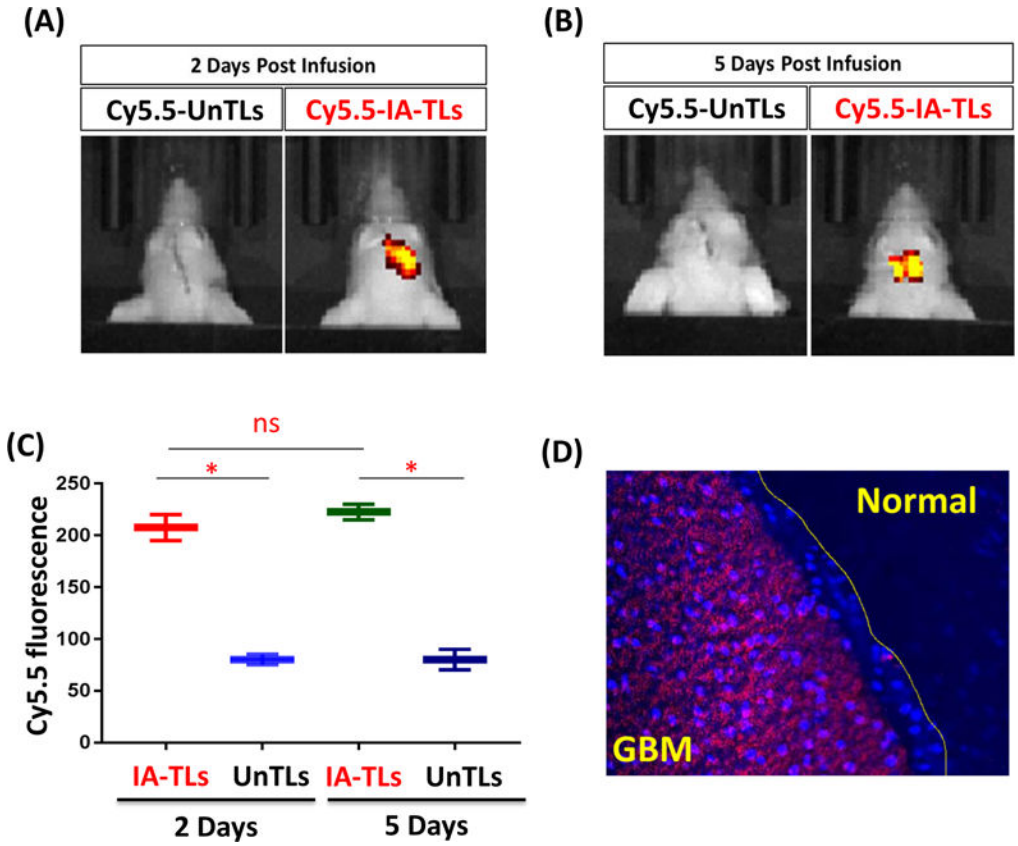

Figure 2. *in vivo* specificity of cy5.5-IA-TLs towards $\alpha_v\beta_3$

in vivo fluorescence imaging showing tumor accumulation of intracranially infused cy5.5 labeled $\alpha_v\beta_3$ targeted nanoparticles (cy5.5-IA-TL) (n=3) and cy5.5 labeled untargeted nanoparticles (n=3) (cy5.5-UnTLs) 2 days (n=3) (A) and 5 days (n=3) (B) post intracranial infusion. (C) Cy5.5-IA-TLs accumulated within GBM tissue significantly greater than cy5.5-UnTLs 2 days and 5 days post intracranial infusion. (D) Brain sections from mice revealed Cy5.5-IA-TLs to be abundant within GBM tissue. Negligible presence of cy5.5-IA-TLs was found within normal regions of the brain surrounding GBM tissue. Data represented as mean +/− SEM. Student's t-test was performed to assess difference between experimental groups (*$p < 0.05$(significant); ns= not significant).

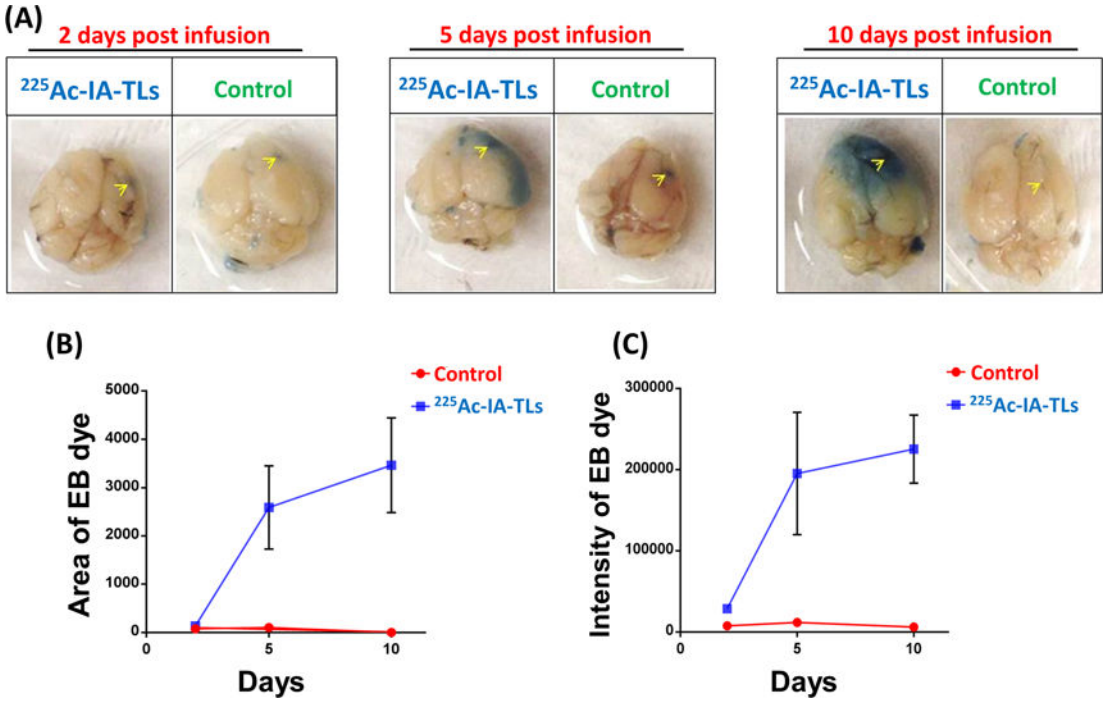

Figure 3. ^{225}Ac-IA-TLs causes BBB opening in immunocompetent mice

(A) Extravasation of intravenously injected Evans blue dye shows clear BBB opening in immunocompetent mice infused with ^{225}Ac-IA-TLs 2 days, 5 Days and 10 days (n=3) when compared to immunocompetent mice that were infused with saline (n=3). Yellow arrows indicate site of intracranial injection. (B) and (C) Area and intensity of extravasated Evans blue dye was also found to be greater in mice intracranially infused with ^{225}Ac-IA-TLs when compared to mice intracranially infused with saline upto 10 days post infusion.

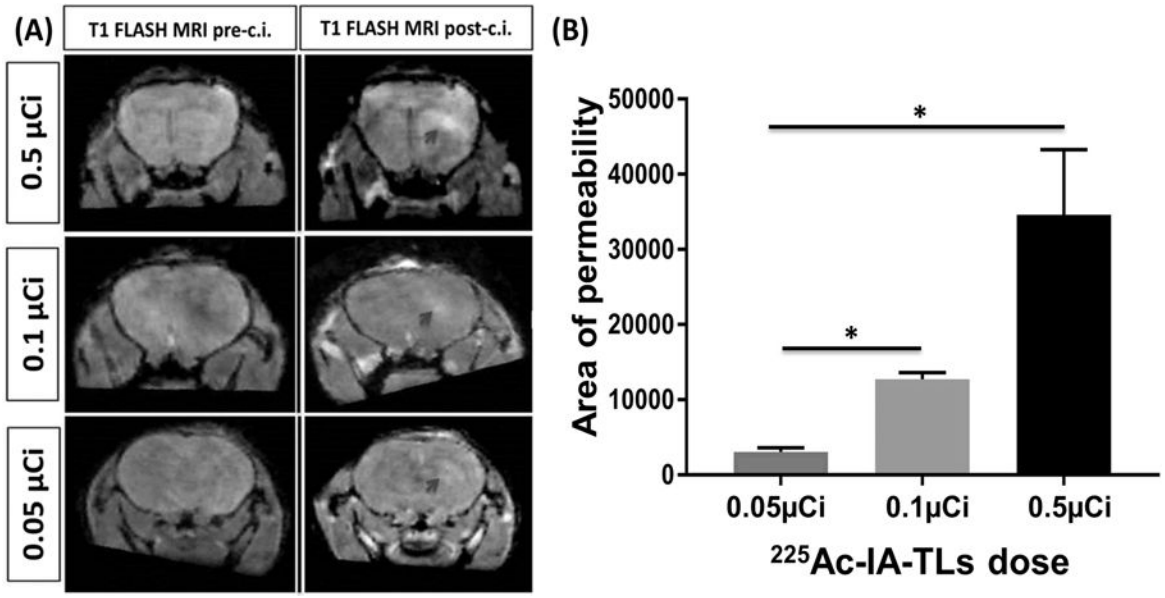

Figure 4. ^{225}Ac-IA-TLs permeabilized BBB in immunocompetent mice in a dose dependent manner

(A) Dose escalation study showed a dose dependent effect of ^{225}Ac-IA-TLs on BBB permeability in immunocompetent mice intracranially infused with ^{225}Ac-IA-TLs (n=15; n=5/dose) indicated by contrast enhancement on MRI. (B) Dose dependent effect of ^{225}Ac-IA-TLs on BBB permeability was also confirmed by the extravasation of intravenously injected Evans Blue dye. Immunocompetent mice intracranially infused with saline showed no BBB opening (n=5). Data represented as mean +/− SEM. Student's t-test and One-way ANOVA was performed to assess differences between experimental groups (*p< 0.05(significant)).

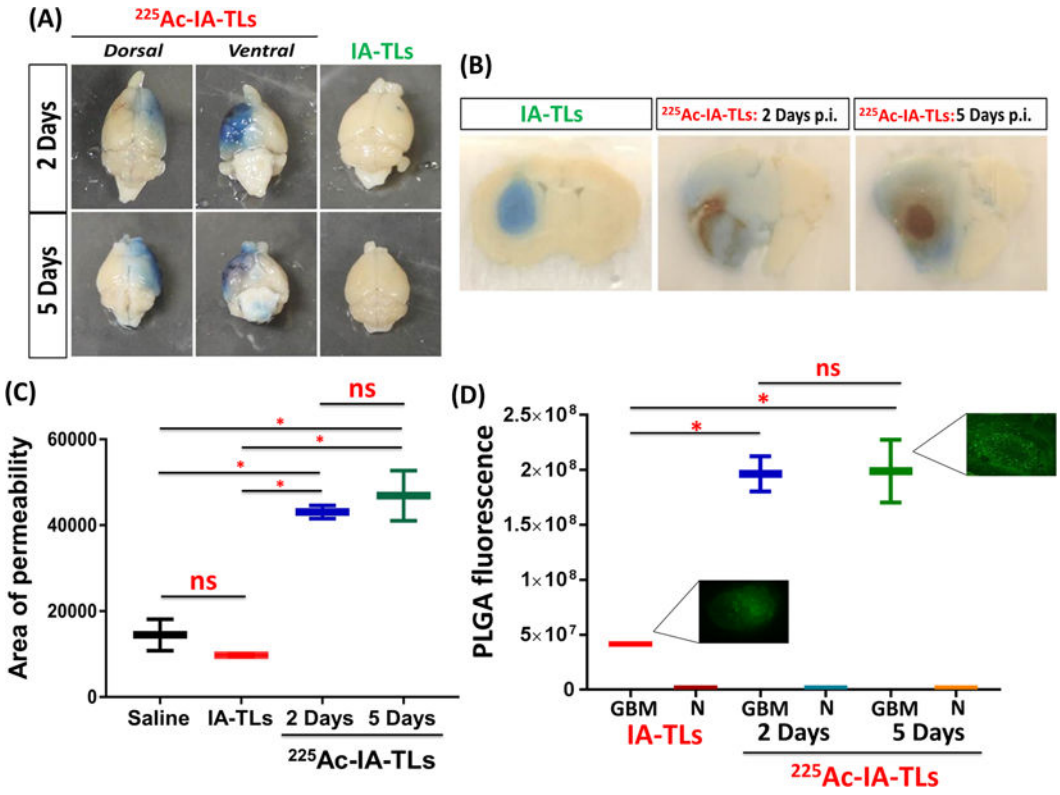

Figure 5. ^{225}Ac-IA-TLs cause significant enhancement of blood-tumor barrier permeability

(A) Extravasation of intravenously injected Evans blue dye showed clear enhancement of blood-tumor barrier permeability in nude mice bearing orthotopic glioblastomas that were intracranially infused with ^{225}Ac-IA-TLs 2 days (n=3) and 5 days (n=3) post infusion when compared to mice bearing orthotopic glioblastomas that were intracranially infused with unlabeled IA-TLs. (B) Brain sections showed extensive enhancement of BTB indicated by the extravasation of Evans blue dye in mice intracranially infused with ^{225}Ac-IA-TLs for a period of 5 days when compared to mice intracranially infused with unlabeled IA-TLs. (C) BTB permeability within untreated GBMs, measured using Evans Blue dye permeabilization was found to be similar in mice intracranially infused with saline and unlabeled IA-TLs. Area of extravasation of Evans Blue dye was significantly greater in brains of mice treated with ^{225}Ac-IA-TLs than in untreated mice. (D) Quantification of systemically injected fluorescent PLGA nanoparticles showed that α- particle enhanced BTB could potentially be exploited to deliver diagnostic and therapeutic agents (n=3/group). PLGA fluorescence in and around GBM tissue was measured. GBM= GBM tissue; N= Normal brain region surrounding GBM tissue. Data represented as mean +/− SEM. Student's t-test and One-way ANOVA was performed to assess differences between experimental groups (*p< 0.001(significant)).

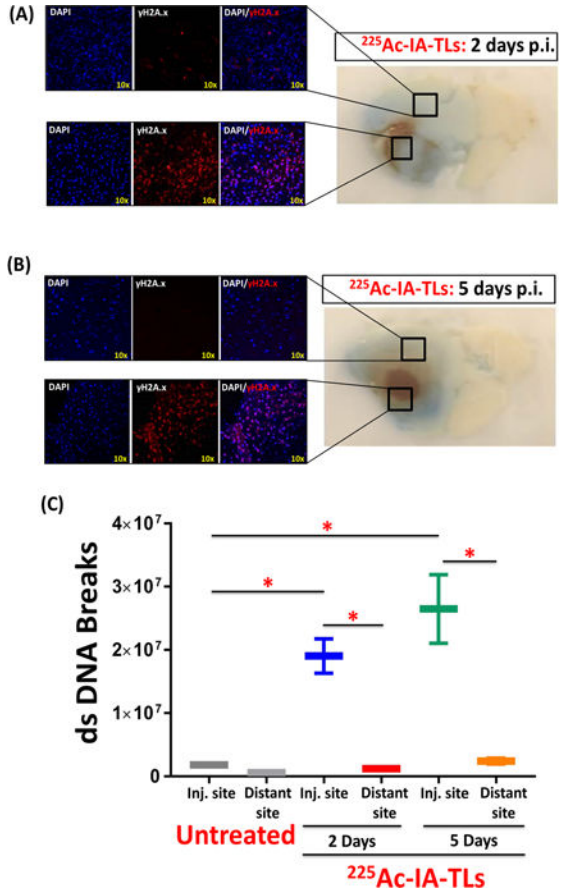

Figure 6. Double strand DNA breaks present within tumor tissue but absent within surrounding tissue showing enhanced vascular permeability

Immunohistochemical staining of sectioned mouse brains revealed the presence of γH2A.X within tumor tissue, indicating α-particle induced tumor cell killing 2 days (n=3) (A) and 5 days (n=3) (B) post intracranial infusion (p.i.) of ^{225}Ac-IA-TLs. (C) Immunohistochemical staining of sectioned mouse brains also revealed negligible presence of γH2A.X in normal brain tissue surrounding tumors (0.5mm from GBM border) (n=3), indicating absence of double strand (ds) DNA breaks within these regions where enhancement in vascular permeability (extravasation of Evans Blue dye) was observed. Data represented as mean +/− SEM. Student's t-test and One-way ANOVA was performed to assess difference between experimental groups (*$p < 0.001$(significant)).